Hyperbranched PEG-based multi-NHS polymer and bioconjugation with BSA

Polymer Chemistry

COMMUNICATION

View Article Online
View Journal | View Issue

Cite this: *Polym. Chem.*, 2017, **8**, 1283

Received 2nd October 2016,
Accepted 22nd December 2016

DOI: 10.1039/c6py01719c

rsc.li/polymers

Hyperbranched PEG-based multi-NHS polymer and bioconjugation with BSA†

Sigen A,‡[a] Qian Xu,‡[a] Dezhong Zhou,[a] Yongsheng Gao,[a] Jeddah Marie Vasquez,[a] Udo Greiser,[a] Wei Wang,*[a,b] Wenguang Liu[b] and Wenxin Wang*[a,b]

Star-shaped poly(ethylene glycol)-*N*-hydroxysuccinimide (star-PEG-NHS) has shown great promise in a variety of biomedical applications owing to its non-toxicity, innate non-immunogenic properties and versatile, multifunctional end groups. However, its complex and sophisticated synthetic methods, as well as high costs, have significantly impeded its wide application. Here, we report the design and synthesis of a hyperbranched PEG-based polymer with multiple NHS functional groups (>12). The hyperbranched PEG-based multi-NHS polymer can react easily with a protein (bovine serum albumin, BSA) to form a PEG-protein hydrogel that displays great potential for biomedical applications.

Star-PEG-NHS (containing 3 or more arms) is one of the most widely used star-PEG polymers for a wide range of biomedical applications owing to the prompt and efficient reaction of the succinimidyl ester and primary amines under physiological conditions. To date, various strategies for the utilization of star-PEG-NHS have been presented in several fields with the aim of applications as a peptide linker[1–4] and in PEGylation,[5–8] cell delivery/cell scaffolds[9–12] and tissue engineering,[13–15] *etc*. Apart from star-PEG-NHS, other multifunctional PEG polymers containing aldehyde groups,[16,17] maleimide groups[18] and epoxy groups[19] have been reported for protein conjugation. An aldehyde group can be coupled with exposed amine groups on proteins to generate an imide bond; a maleimide group can readily undergo conjugate addition with α,β-unsaturated carbonyl compounds to produce a thioether bond with a cysteine residue bearing a thiol group in proteins; and materials containing epoxy groups can also be used for protein conjugation owing to the nucleophilicity of the amine groups in proteins. However, there are some drawbacks of these conjugation methods such as the high cytotoxicity of the aldehyde group,[19] extremely low reactivity of the epoxy group[20] and slow hydrolysis of the maleimide bond under aqueous conditions, which may result in problems during the handling of proteins.[20] These drawbacks make star-PEG-NHS polymers more appealing for protein conjugation. Nevertheless, the preparation of star-PEG polymers still requires complicated synthetic strategies, which are the main reason why the high costs of star-PEG polymers adversely affect the further successful commercialisation of star-PEG polymers. Furthermore, to the best of our knowledge, there has been no report of the synthesis of star-PEG polymers with a number of terminal NHS functional groups in excess of 8 yet. It can be expected that a higher amount of NHS functional groups would result in more efficient and faster conjugation between NHS and primary amine groups. Thus, the development of new approaches for constructing multi-armed PEG-based polymers *via* a simpler and more straightforward synthetic pathway, as well as tuneable arm structures, is of great importance.

Hyperbranched biopolymers are a special class of synthetic biomaterials with three-dimensional (3D) architectures containing highly branched side chains. These unique features provide these polymers with the following particular structures and properties: multiple end functional groups; structures with cavities within the polymer frameworks; relatively lower viscosity owing to lower chain entanglement in comparison with linear polymers; and also high solubility in various organic and inorganic solvents. Previously, our laboratory had demonstrated several novel synthetic approaches for building hyperbranched polymers by the controlled/living radical polymerisation of multi-vinyl monomers (MVMs),[21,22] which was termed the 'vinyl oligomer combination' strategy. At the early stage of polymerisation, linear oligomers with terminal acrylate groups are formed by the slow chain growth of divinyl monomers. Then, these linear oligomer chains combine *via* the terminal acrylate groups of other linear oligomers to form highly branched polymers. The dense vinyl groups in the polymer backbone not only render this class of hyperbranched

[a]*Charles Institute of Dermatology, School of Medicine, University College Dublin, Dublin 4, Ireland*
[b]*School of Materials Science and Engineering, Tianjin Key Laboratory of Composite and Functional Materials, Tianjin University, Tianjin 300350, China.*
E-mail: wenxin.wang@ucd.ie, wwgfz@tju.edu.cn

†Electronic supplementary information (ESI) available. See DOI: 10.1039/c6py01719c

‡These authors contributed equally to this work.

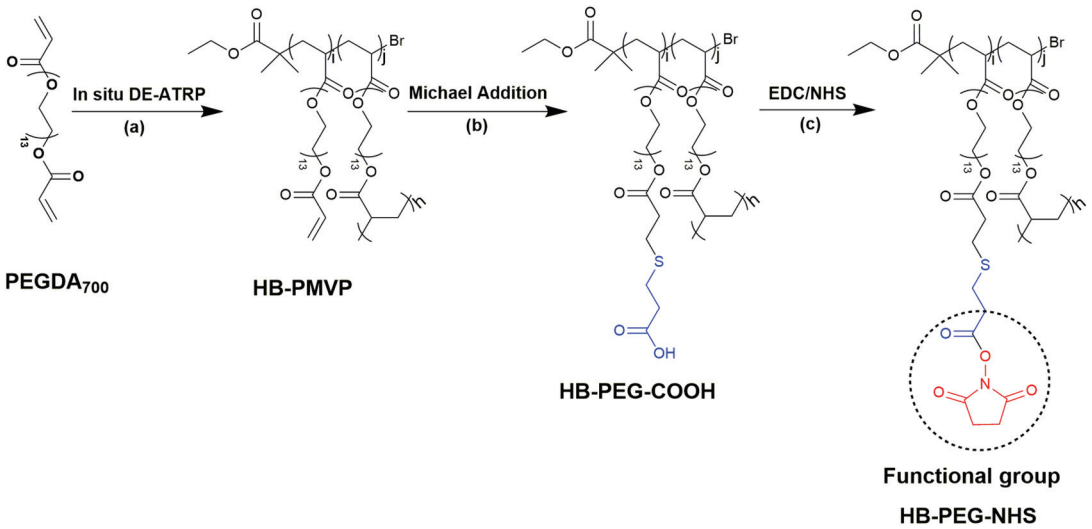

Scheme 1 Synthetic pathway of HB-PEG-NHS. (a) *In situ* DE-ATRP of $PEGDA_{700}$. [I] : [PEGDA] : [$CuCl_2$] : [L] : [R] = 1 : 3 : 0.025 : 0.025 : 0.0125. I: ethyl 2-bromoisobutyrate, L: 1,1,4,7,7-pentamethyldiethylenetriamine, R: ascorbic acid, T = 50 °C; (b) $NaHCO_3$, 60 °C, 3-mercaptopropionic acid; (c) 1-ethyl-3-(3-dimethylaminopropyl)carbodiimide (EDC), *N*-hydroxysuccinimide (NHS), RT.

polymers an ideal matrix for post-functionalisation, but also provide various possibilities of fabricating multi-armed PEG polymers with different functional groups.

Herein, a novel NHS-modified hyperbranched polymer synthesized by post-functionalisation of a hyperbranched poly(multi-vinyl) polymer (HB-PMVP) is reported. As outlined in Scheme 1, the newly designed HB-PMVP was synthesized *via in situ* deactivation-enhanced atom transfer radical polymerisation (DE-ATRP). The modification process included two steps (Scheme 1b and c): (1) end-capping of the vinyl group with 3-mercaptopropionic acid (3-MA); and (2) conjugation of the carboxyl group with NHS.

Firstly, *in situ* DE-ATRP was conducted using poly(ethylene oxide) diacrylate (PEGDA, M_n = 700 Da) as the monomer, and the M_w of HB-PMVP was monitored by GPC (Fig. S1 and Table S1, ESI†). The polymerisation reaction displayed a controlled behaviour as demonstrated by the kinetics plot. Specifically, the recorded kinetics plot is first-order with respect to conversion of the monomer, which demonstrates living polymerization, and K_p^{app} was found to be 0.003 min^{-1} (Fig. S2 and S3, ESI†). The reaction was stopped when propagation of the polymer started to accelerate, in order to avoid large-scale intermolecular crosslinking during the later stage of polymerisation (Fig. S2, ESI†). According to our previous research, the molecular weight, branching degree, and vinyl content of HB-PMVP can be regulated simply by adjusting the ratio of the initiator to the monomer or the polymerisation time.[21,22] It is commonly known that there are two types of crosslinking pathway during the homopolymerisation of multi-vinyl monomers: intramolecular crosslinking, which accounts for the formation of 'loops' in the polymer structure, and intermolecular combination, which leads to propagation of the polymer chain *via* combination of macromers. Disparate polymer structures can be obtained by properly adjusting the ratio of the initiator and monomer. A larger amount of the initiator in the polymerisation process can largely suppress intramolecular crosslinking while promoting intermolecular combination, which leads to a highly branched structure, whereas the use of a lower amount of the initiator can enhance intramolecular crosslinking to form a knot structure. In this study, a high molar ratio of initiator to monomer (1 : 3) was employed in order to obtain a hyperbranched polymer with a higher content of vinyl groups for the subsequent modification process. HB-PMVP with an intermediate branching degree of 38% and a molecular weight of 12 kDa was used for the subsequent investigation. The structure of HB-PEG-NHS was confirmed by ^{1}H-NMR (Fig. 1a) and GPC (Fig. 1b and Table S2, ESI†). The results of ^{1}H-NMR (Fig. 1a) show that the three peaks around 5.8–6.4 ppm disappeared after the end-capping step, which indicated that all vinyl groups in HB-PMVP were fully consumed during the end-capping reaction. Moreover, a single peak can be observed at 2.8 ppm, which indicates that the NHS group was conjugated to the polymer backbone successfully after the second step of modification. In order to further confirm the success of the modification steps, the ^{13}C-NMR spectra of HB-PMVP and HB-PEG-NHS were recorded (Fig. S6†). The two vinyl peaks at 128 and 131 ppm in the spectrum of HB-PMVP disappeared after the end-capping reaction with 3 MPA, which is consistent with the result of ^{1}H-NMR that the vinyl groups were fully consumed. The two peaks at 169 and 171 ppm were attributed to the carbonyl groups of 3 MPA and NHS units, respectively.

We also investigated the α parameter of the polymers pre- and post-modification (Fig. 1c, Table S2, ESI†). According to the Mark–Houwink equation, a value of α of less than 0.5 indicates a branched or spherical macromolecular structure.[23] Here, the α values of HB-PMVP and HB-PEG-NHS are 0.32 and 0.34, respectively (Fig. 1c, Table S2, ESI†), which illustrates the

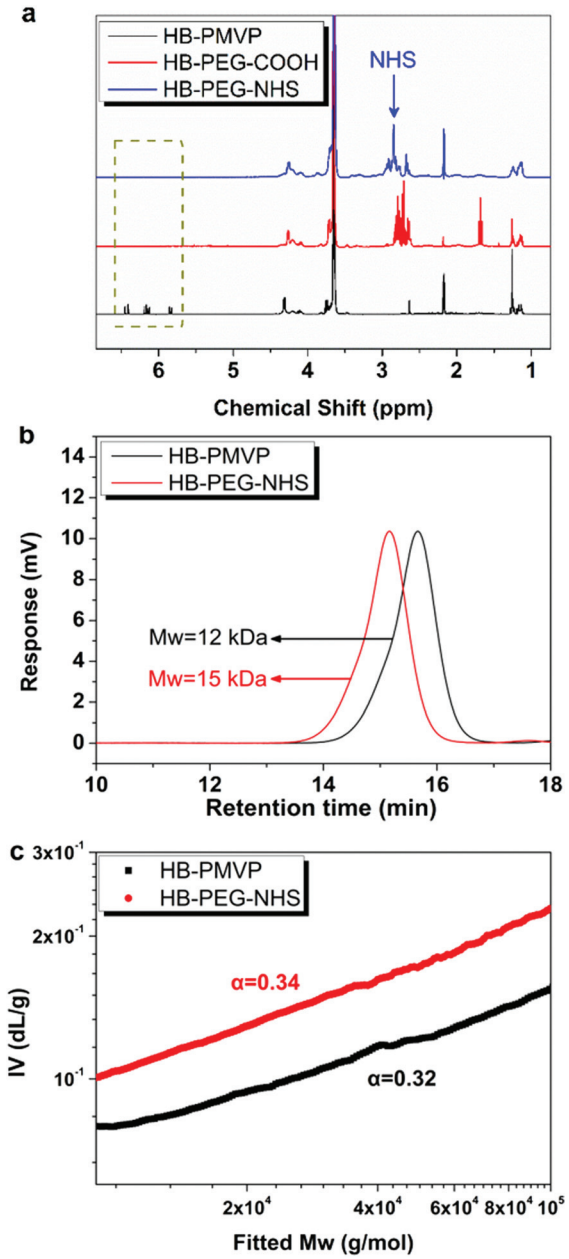

Fig. 1 (a) ^{1}H-NMR results for purified HB-PMVP (black), HB-PEG-COOH (red), and HB-PEG-NHS (blue). (b) GPC traces pre- and post-modification for HB-PMVP (black) and HB-PEG-NHS (red). (c) Mark–Houwink (MH) plots and α values of HB-PMVP and HB-PEG-NHS.

branched topology of the structure. Moreover, the branched structure was preserved after the modification process. To confirm this result, the branching degree was calculated from the results of ^{1}H-NMR (Table S2, ESI†). The branching degree of HB-PMVP was very close to that obtained for HB-PEG-NHS (38% *vs.* 40%, Fig. S4†), which supports the conclusion that the structure of the polymer framework was maintained after modification.

On the basis of the results of NMR and GPC tests, the content of NHS functional groups in each HB-PEG-NHS polymer chain is 0.85 mmol g^{-1} (cal. 12.8 NHS groups per polymer chain, Fig. S5†). To confirm this result, a modified Ellman assay was conducted to quantify the NHS content in the HB-PEG-NHS polymer. As can be seen from Fig. S7,† the NHS content is up to 0.92 mmol g^{-1} (cal. 13.9 NHS groups per polymer chain), which is very close to the results obtained from NMR and GPC tests. Notably, it is much higher than the contents of 0.2 mmol g^{-1} and 0.4 mmol g^{-1} of the most widely used 20 kDa 4-arm and 8-arm forms of star-PEG-NHS (Creative PEGWorks product codes: PSB-487 and PSB-847 for 4-arm PEG-NHS and 8-arm PEG-NHS, respectively. Price: US $300 per gram.), respectively. Obviously, our HB-PEG-NHS contains a much larger amount of NHS than all the other commercial products.

Considering the abundant NHS groups in the polymer backbone, a hydrogel system was developed based on HB-PEG-NHS and bovine serum albumin (BSA). BSA, which is known as Fraction V, has been widely used in biochemistry because of its relative stability and low price.

With the aim of determining the mechanical properties of the PEG-BSA hydrogels, detailed dynamic rheological assessments were conducted on hydrogels of two concentrations (Hydrogel-H: 10% HB-PEG-NHS + 15% BSA; Hydrogel-L: 5% HB-PEG-NHS + 15% BSA). Firstly, the results of frequency sweep tests (Fig. 2a) demonstrated that both hydrogels possessed higher storage moduli (G') than loss moduli (G'') at all frequencies in the range from 0.1 to 100 Hz, which indicates the formation of solid chemically crosslinked hydrogels. In addition, a nearly fourfold increase in G' can be seen as the concentration of HB-PEG-NHS increased from 5% (2.3 ± 0.4 kPa) to 10% (8.3 ± 1.4 kPa), which can be attributed to an increasing degree of crosslinking. Adjustable stiffness properties are desired, because the stiffness of a hydrogel plays a key role in biological applications. For instance, it can not only manipulate cell differentiation but also affect cell activity when the hydrogel is used as a 3D cell culture scaffold.[24,25] In addition, the stiffness must be comparable to that of the surrounding tissue if the hydrogel is applied as a tissue adhesive. A weak hydrogel may provide insufficient supporting strength to the surrounding tissue, whereas a rigid hydrogel may result in tissue damage or disturbance to the internal pressure. Afterwards, strain sweep tests were performed over the strain range between 0.1% and 100%. Hydrogel-L displayed excellent strain-resistant properties over the entire testing range, whereas the G' value of Hydrogel-H slightly decreased in the high-strain region (Fig. 2b), which illustrated that the brittleness of the hydrogel increased in conjunction with the increasing concentration of HB-PEG-NHS.

In order to investigate whether or not the NHS groups were fully consumed in the crosslinked hydrogels, a modified Ellman assay was conducted. The reduction of thiol groups was converted into the percentage of free NHS groups in the hydrogel, which was found to be less than 1% for Hydrogel-L and 19.6% for Hydrogel-H (Fig. S8†).

To determine the biocompatibility of the HB-PEG-NHS-BSA hydrogel, the cell viability of cells embedded into the hydrogel

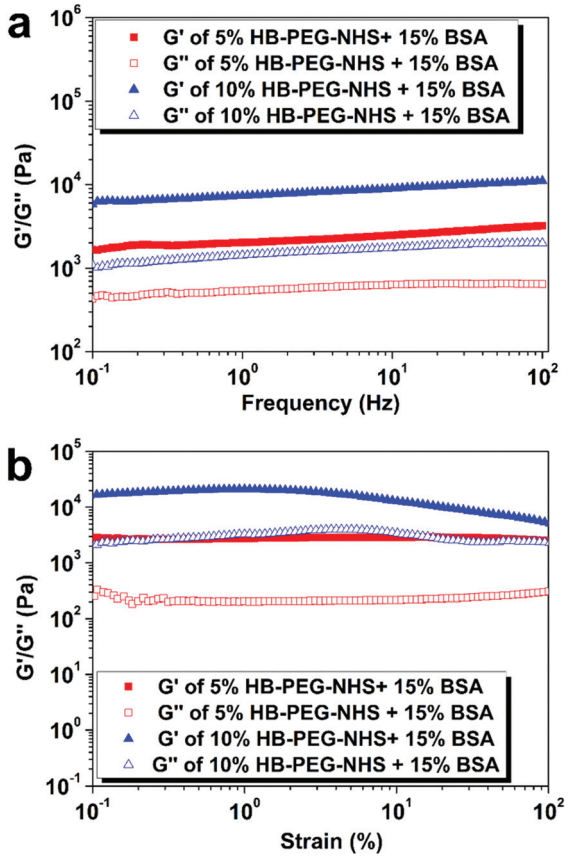

Fig. 2 Rheological assessment of PEG-BSA hydrogels. The red lines represent PEG-BSA hydrogel with a final concentration of 5% HB-PEG-NHS and 15% BSA, whereas the blue lines represent PEG-BSA hydrogel with a final concentration of 10% HB-PEG-NHS and 15% BSA; the solid symbols represent storage moduli *G'* and the hollow symbols represent loss moduli *G''*. (a) Frequency sweep tests from 0.1 to 100 Hz. (b) Strain sweep tests over the range of 0.1–100%.

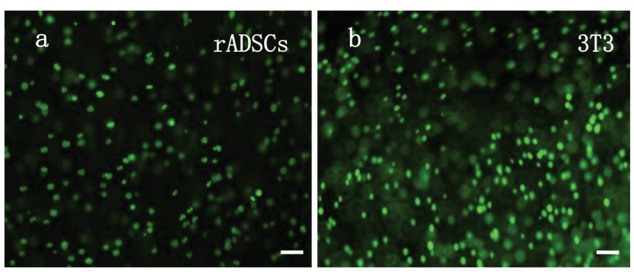

Fig. 3 Cell viability assessment of Hydrogel-L (5% HB-PEG-NHS + 15% BSA) using a LIVE/DEAD assay up to 48 h: (a) Hydrogel-L embedded with rADSCs; (b) Hydrogel-L embedded with 3T3 fibroblasts. The scale bars represent 100 μm in both cases.

(LIVE/DEAD assay) and the cytotoxicity of the HB-PEG-NHS polymer (MTT assay) were determined using 3T3 fibroblasts and rat adipose-derived stem cells (rADSCs). The viability of both cell types was well maintained after culture for 48 hours (Fig. 3). The results of the MTT assays demonstrate that the viability rADSCs did not exhibit a significant difference at any concentration in comparison to the control group (Fig. S9†). As for the 3T3 fibroblasts, the cell viability decreased slightly to 86% at a concentration of 1000 μg mL^{-1}, which is still considered to show the non-cytotoxic effect of the polymer. The high biocompatibility can be mainly attributed to the PEG-based framework. It is also worth noting that the introduction of carboxyl and NHS motifs did not increase the cytotoxicity of the material.

In summary, a newly designed hyperbranched PEG-based multi-NHS polymer was successfully synthesized. The polymer possesses an easily tuneable chemical structure (*e.g.*, molecular weight, branching degree and backbone structure) and a high density of functional groups, as well as negligible cytotoxicity, owing to its PEG-based skeleton. Moreover, its ability to form a hydrogel with BSA shows that HB-PEG-NHS may be a potential substitute for glutaraldehyde. These properties suggest that the HB-PEG-NHS polymer should be a promising material for various biological applications. In addition, we have demonstrated a novel synthetic strategy for constructing hyperbranched polymers with different functionalities. Currently, the design and synthesis of hyperbranched polymers bearing various functional groups, including aldehyde, amino and thiol groups, are ongoing in our laboratory.

According to the reference, all animal experimental protocols were approved by the Animal Care and Research Ethics Committee of the National University of Ireland, Galway (No. 009/10(B)) and were conducted under an animal license (No. B100/4342) authorized by the Irish Department of Health and Children. Animal care was in compliance with the standard operating procedures of the Animal Facility at the National Centre for Biomedical Engineering Science, NUIG. The murine 3T3 fibroblast cell line was purchased from Sigma-Aldrich.

Acknowledgements

This work was funded by Science Foundation Ireland (SFI), grant number 13/IA/1962 (SFI Principal Investigator Award), grant number 12/IP/1688 (SFI Principal Investigator Program), grant number HRA-POR-2013-412 (Health Research Award from the Health Research Board of Ireland), grant number 14/TIDA/2367 (Technology Innovation and Development Award), grant number 15/IFA/3037 (Industry Fellowship), University College Dublin and DEBRA Ireland, National Natural Science Foundation of China (Grant No. 51473117), and Tianjin Municipal Natural Science Foundation (Grant No. 15JCQNJC03300).

Notes and references

1 M. V. Tsurkan, K. Chwalek, K. R. Levental, U. Freudenberg and C. Werner, *Macromol. Rapid Commun.*, 2010, **31**, 1529.
2 A. Sugiyama, A. Sato, H. Shimizu, K. Ando and T. Takeuchi, *J. Vet. Med. Sci.*, 2010, **72**, 173.

3 B. P. Ting, J. Zhang, Z. Gao and J. Y. Ying, *Biosens. Bioelectron.*, 2009, **25**, 282.
4 S. A. DeLong, J. J. Moon and J. L. West, *Biomaterials*, 2005, **26**, 3227.
5 P. K. Thalla, A. Contreras-Garca, H. Fadlallah, J. Barrette, G. De Crescenzo, Y. Merhi and S. Lerouge, *BioMed Res. Int.*, 2013, **2013**, 1.
6 Y. Nojima, K. Iguchi, Y. Suzuki and A. Sato, *Biol. Pharm. Bull.*, 2009, **32**, 523.
7 D. I. Lee, C. J. Kim, C. H. Lee and I. S. Ahn, *J. Ind. Eng. Chem.*, 2012, **18**, 1186.
8 M. J. Joralemon, S. McRae and T. Emrick, *Chem. Commun.*, 2010, **46**, 1377.
9 G. Fontana, D. Thomas, E. Collin and A. Pandit, *Adv. Healthcare Mater.*, 2014, **3**, 2012.
10 D. Thomas, G. Fontana, X. Chen, C. Sanz-Nogus, D. I. Zeugolis, P. Dockery, T. O'Brien and A. Pandit, *Biomaterials*, 2014, **35**, 8757.
11 U. Freudenberg, A. Hermann, P. B. Welzel, K. Stirl, S. C. Schwarz, M. Grimmer, A. Zieris, W. Panyanuwat, S. Zschoche, D. Meinhold, A. Storch and C. Werner, *Biomaterials*, 2009, **30**, 5049.
12 H. Tan, A. Defail, J. P. Rubin, C. R. Chu and G. Kacey, *J. Biomed. Mater. Res., Part A*, 2011, **92**, 979.
13 G. N. Grover, N. Rao and K. L. Christman, *Nanotechnology*, 2014, **25**, 014011.
14 E. C. Collin, S. Grad, D. I. Zeugolis, C. S. Vinatier, J. R. Clouet, J. J. Guicheux, P. Weiss, M. Alini and A. S. Pandit, *Biomaterials*, 2011, **32**, 2862.
15 L. S. Kontturi, E. Järvinen, V. Muhonen, E. C. Collin, A. S. Pandit, I. Kiviranta, M. Yliperttula and A. Urtti, *Drug Delivery Transl. Res.*, 2014, **4**, 149.
16 G. MacBeath and S. L. Schreiber, *Science*, 2000, **289**, 1760.
17 T. Viitala, I. Vikholm and J. Peltonen, *Langmuir*, 2000, **16**, 4953.
18 C. Mateo, O. Abian, G. Fernandez-Lorente, J. Pedroche, R. Fernandez-Lafuente and J. M. Guisan, *Biotechnol. Prog.*, 2002, **18**, 629.
19 R. LoPachin and T. Gavin, *Chem. Res. Toxicol.*, 2014, **27**, 1081.
20 F. Rusmini, Z. Zhong and J. Feijen, *Biomacromolecules*, 2007, **8**, 1775.
21 T. Zhao, Y. Zheng, J. Poly and W. Wang, *Nat. Commun.*, 2013, **4**, 1873.
22 T. Zhao, H. Zhang, D. Zhou, Y. Gao, Y. Dong, U. Greiser, H. Tai and W. Wang, *RSC Adv.*, 2015, **5**, 33823.
23 L. H. Sperling, *Introduction to physical polymer science*, 2005, vol. 31.
24 T. C. Tseng, L. Tao, F. Y. Hsieh, Y. Wei, I. M. Chiu and S. H. Hsu, *Adv. Mater.*, 2015, **27**, 3518.
25 O. Chaudhuri, L. Gu, D. Klumpers, M. Darnell, S. A. Bencherif, J. C. Weaver, N. Huebsch, H.-P. Lee, E. Lippens, G. N. Duda and D. J. Mooney, *Nat. Mater.*, 2015, **15**, 326.